0026-895X/02/6206-1418–1430$7.00
MOLECULAR PHARMACOLOGY
Copyright © 2002 The American Society for Pharmacology and Experimental Therapeutics
Mol Pharmacol 62:1418–1430, 2002

Vol. 62, No. 6
1848/1025110
Printed in U.S.A.

Characteristics of Block by Pb^{2+} of Function of Human Neuronal L-, N-, and R-Type Ca^{2+} Channels Transiently Expressed in Human Embryonic Kidney 293 Cells

SHUANGQING PENG, RAVINDRA K. HAJELA, and WILLIAM D. ATCHISON

Department of Pharmacology and Toxicology, Institute of Environmental Toxicology and Neuroscience Program, Michigan State University, East Lansing, Michigan

Received May 13, 2002; accepted September 4, 2002

This article is available online at http://molpharm.aspetjournals.org

ABSTRACT

Lead (Pb^{2+}) is a well-known inhibitor of voltage-dependent Ca^{2+} channels in their native environments in several types of cells. However, its effects on discrete Ca^{2+} channel phenotypes in isolation have not been well studied. We compared how specific subtypes of human neuronal high-voltage–activated Ca^{2+} channels were affected by acute exposure to Pb^{2+}. Expression cDNA clones of human α_{1C}, α_{1B}, or α_{1E} subunit genes encoding neuronal L-, N-, and R-subtypes of Ca^{2+} channels, respectively, along with a constant $\alpha_2\delta$ and β_3 subunits were transfected into human embryonic kidney 293 cells. Currents through the respective transiently expressed channels were measured using whole-cell recording techniques with Ba^{2+} (20 mM) as charge carrier. Extracellular bath applications of Pb^{2+} significantly reduced current amplitude through all three types of Ca^{2+} channels in a concentration-dependent manner. The order of potency was: α_{1E} (IC_{50} = 0.10 μM), followed by α_{1C} (IC_{50} = 0.38 μM) and α_{1B} (IC_{50} = 1.31 μM). Pb^{2+}-induced perturbation of function of α_{1C} and α_{1B} containing Ca^{2+} channels was more easily reversed than for α_{1E}-containing Ca^{2+} channels after washing with Pb^{2+} free solution. The current-voltage relationships were not altered after 3-min exposure to Pb^{2+} for any of the three types. However, the steady-state inactivation relationships were shifted to more negative potentials for channels containing α_{1B} and α_{1E} subunits, but not for those containing α_{1C} subunits. Pb^{2+} accelerated the inactivation time of current in all three subtypes of Ca^{2+} channels in a concentration- and voltage-dependent manner. Therefore, different subtypes of Ca^{2+} channels exhibit differential susceptibility to Pb^{2+} even when expressed in the same cell type. Current expressed by α_{1E}-containing channels is more sensitive to Pb^{2+} than that expressed by α_{1C}- or α_{1B}-containing channels. Several Ca^{2+} channel phenotypes are quite sensitive to the inhibitory action of Pb^{2+}. Furthermore, it seems that Pb^{2+} is more likely to combine with Ca^{2+} channels in the closed state.

Voltage-sensitive Ca^{2+} channels regulate a number of critical cellular functions in the nervous system, such as synaptic transmission (Catterall, 2000). Several distinct subtypes of neuronal "high-voltage–activated" Ca^{2+} channels (L, N, P/Q, and R) have been identified based on their biophysical and pharmacological properties (Tsien et al., 1995). These channels consist of four subunits: α_1, β, α_2, and δ; the α_1 subunit is the pore-forming, voltage-sensing, ligand-binding, and subtype-determining moiety (Hofmann et al., 1999). At least six distinct α_1 subunits have been cloned for high-voltage–activated Ca^{2+} channels, encoding α_{1A}, α_{1B}, α_{1C}, α_{1D}, α_{1E}, and α_{1S} phenotypes. Expression studies have shown that α_{1C}, α_{1D}, and α_{1S} phenotypes encode dihydropyridine-sensitive Ca^{2+} channels (L-type) (Williams et al., 1992a; Tomlinson et al., 1993), α_{1B} encodes ω-conotoxin GVIA-sensitive Ca^{2+} channels (N-type) (Williams et al., 1992b; Cahill et al., 2000), α_{1A} encodes ω-agatoxin IVA-sensitive Ca^{2+} channels (P/Q-type) (Mori et al., 1991; Stea et al., 1994), and α_{1E} encodes Ca^{2+} channels resistant to most currently known specific inhibitors (R-type) (Williams et al., 1994; Bourinet et al., 1996), but partially susceptible to a tarantula spider toxin SNX 482 (Bourinet et al., 2001) and evidently also susceptible to block by Cd^{2+}. Four different β subunits—β_1 to β_4—and two different α_2 subunits serve to regulate assembly and modulate the kinetic parameters of the channels. Each of these subunit types can also have various isoforms and splice variants, further complicating the functional expression characteristics and classification (Brust et al., 1993; De Waard and Campbell, 1995; McEnery et al., 1998; Pan and Lipscombe, 2000). Because of their portal

This work was supported by National Institute of Environmental Health Sciences grant ES05822.

Preliminary reports of some of these results were presented at the 40th Annual Meeting of the Society of Toxicology, 2001 March 25–29, San Francisco, CA (published in abstract form in *The Toxicologist* **60:**185) and the 31st Annual Meeting of the Society For Neuroscience, 2001 Nov 10–15, San Diego, CA (published in abstract form in *Soc Neurosci Abstr* **27**.

ABBREVIATIONS: HEK, human embryonic kidney; GFP, green fluorescent protein.

location within the plasma membrane, Ca^{2+} channels are readily exposed to toxicants, and are potentially early targets of the actions of a number of toxicants (Kiss and Osipenko, 1994). In view of the crucial roles that Ca^{2+} channels play in key cellular functions, toxicant effects on Ca^{2+} channels could have significant deleterious consequences for cell function.

Lead (Pb^{2+}) is a commonly occurring and persistent environmental neurotoxicant that causes block of function of voltage-activated Ca^{2+} channels (Audesirk and Audesirk, 1989, 1991; Reuveny and Narahashi, 1991; Oortgiesen et al., 1993) and evidently uses these channels as a means of entry into cells (Simons and Pocock, 1987). Inhibitory effects of acute exposure to Pb^{2+} on native Ca^{2+} channels have been reported for invertebrate neurons (Audesirk and Audesirk, 1989; Büsselberg et al., 1991), rat dorsal root ganglion neurons (Evans et al., 1991; Büsselberg et al., 1994) pheochromocytoma cells (PC12) (Hegg and Miletic, 1996, 1998; Shafer, 1998), mouse and human neuroblastoma (Audesirk and Audesirk, 1991; Reuveny and Narahashi, 1991; Oortgiesen et al., 1993), and bovine chromaffin cells (Tomsig and Suszkiw, 1991; Sun and Suszkiw, 1995). However, although different cell types show apparently differential sensitivity to Pb^{2+}, there are very few reports on the effects of Pb^{2+} on specific defined subtypes of Ca^{2+} channels, and there are no comparative studies using recombinant channels to test for differences among distinct Ca^{2+} channel phenotypes. Moreover, despite the clear neurotoxicity of Pb^{2+}, there are no reports of effects of the metal on heterologously-expressed cloned neuronal Ca^{2+} channels, although Bernal et al. (1997) reported that Pb^{2+} suppressed the function of stably expressed L-type cardiac Ca^{2+} channels from rabbit. The objective of the present study was to compare and characterize the acute effects of Pb^{2+} on isolated, distinct phenotypes of voltage-activated Ca^{2+} channels typically expressed in neurons. Because of the multitude of intracellular actions that Pb^{2+} has, many of which could influence Ca^{2+} channel function, such as its well-known interaction with protein kinase C (Markovac and Goldstein, 1988), we limited the comparison to effects that are likely to occur solely at the membrane level to eliminate the confounding problem of possible interaction of Pb^{2+} with specific intracellular components of the channel. As such, we used a single, constant β subunit. We discuss how the effects of Pb^{2+} on recombinant channels compare with those presumably similar channel phenotypes (based on pharmacological sensitivities) when expressed in a native setting. Transiently expressed human neuronal voltage-dependent Ca^{2+} channels were used to examine toxic effects of Pb^{2+} as applied acutely in the extracellular solution on one specific subtype of Ca^{2+} channel at a time. Expression cDNA clones of α_{1C}, α_{1B}, or α_{1E} subunits coding for neuronal L-, N-, and R-subtypes, respectively, were combined with a constant $\alpha_2\delta$ and β_3 Ca^{2+} channel subunits of human neuronal origin to transfect human embryonic kidney (HEK) 293 cells. Jellyfish green fluorescent protein (GFP) was used as a cotransfection reporter. Characteristics of current conducted through each channel subtype as well as the effects of Pb^{2+} on that current were examined after transient transfection using whole-cell, voltage-clamp recording techniques and Ba^{2+} as charge carrier.

Materials and Methods

Materials. HEK 293 cells were purchased from the American Type Culture Collection (Manassas, VA). All reagents were pure or ultrapure laboratory grade unless specifically noted. ATP-Mg, cAMP, HEPES, EGTA, and tetrodotoxin were all obtained from Sigma Chemical Co. (St. Louis, MO). Stock solutions (10 mM) of lead acetate (J. T. Baker Chemical Co., Phillipsburg, NJ) were prepared weekly in double-distilled water, from which test solutions were prepared in extracellular solution just before each experiment. Expression cDNA clone plasmids of human neuronal Ca^{2+} channel subunits used in the study were all generously provided by Dr. Kenneth A. Stauderman of SIBIA Neurosciences (San Diego, CA), now Merck Research Laboratories. The human gene source tissues were as follows: $\alpha_{1B\text{-}1}$, neuroblastoma cell line IMR32 (Williams et al., 1992b); $\alpha_{1C\text{-}1}$, hippocampus (M. E. Williams, unpublished observations); $\alpha_{1E\text{-}3}$, hippocampus (Williams et al., 1994); $\alpha_2\delta$, brainstem and basal ganglia (Williams et al., 1992a); and β_3, hippocampus (M. E. Williams, unpublished observations). GFP sequences were removed from pEGFP-1 (BD Biosciences Clontech, Palo Alto, CA) and subcloned in pCDNA3.1 (Invitrogen, Carlsbad, CA) in our laboratory.

Cell Culture and Transfection. HEK 293 cells were grown at 37°C in Eagle's minimal essential medium fortified with 1 mM sodium pyruvate, 0.1 mM nonessential amino acids, 2 mM L-glutamine, 1.5 g/l sodium bicarbonate, 10% (w/v) fetal bovine serum, and penicillin, streptomycin, and antimycotic mixture (final concentrations: 100 U/ml penicillin; 100 μg/ml streptomycin; and 0.25 μg/ml amphotericin B as Fungizone) (Invitrogen) in a 5% CO_2 environment. One day before gene transfer, cells were plated at a density of 5×10^5 on 35-mm culture dishes. Cells were transfected with a mixture of plasmids containing either $\alpha_{1B\text{-}1}$, $\alpha_{1C\text{-}1}$, or $\alpha_{1E\text{-}3}$ Ca^{2+} channel subunits together with $\alpha_{2b}\delta$, β_{3a}, and the GFP cDNA clone, using Fugene 6 (Roche Molecular Biochemicals, Indianapolis, IN) following the manufacturer's instructions. Reactions contained a total of 3 μl of Fugene 6 and 1 μg of plasmid DNA containing the three channel subunits in 1:1:1 M ratio, with GFP plasmid at 20% of the total DNA. Two days were allowed for optimal, transient expression of proteins, at which time the cells were examined for GFP expression. Cells from dishes with a number of green fluorescent cells were replated at a low density to isolate a population of individual cells and allowed to recover at least 2 h to facilitate recording. Recordings were typically made from cells from a minimum of three independent transfections.

Ca^{2+} Channel Current Recording. Before recording, culture medium was removed, cells were rinsed twice with extracellular solution and then replenished with 1 ml of extracellular recording bath solution. The extracellular solution contained 117 mM tetraethylammonium chloride, 20 mM $BaCl_2$, 1 mM $MgCl_2$, 25 mM D-glucose, 10 mM HEPES, and 0.001 mM tetrodotoxin, pH adjusted to 7.2 at room temperature (23–25°C) using tetraethylammonium hydroxide. Ba^{2+} was used as charge carrier because in control experiments, amplitudes of currents carried by Ca^{2+} varied significantly among cells of the different phenotypes (results not shown). Thus a constant $[Ba^{2+}]_e$ was used to allow results to be compared across phenotypes more readily. Patch-clamp pipettes with resistance between 6 and 8 MΩ were prepared from glass capillaries (1.5-mm i.d.; World Precision Instruments, New Haven, CT) using a two-stage microelectrode puller (PP-830; Narishige, Tokyo, Japan) and fire-polished using a Narishige MF-830 microforge. Intracellular (pipette) solution contained 140 mM CsCl, 10 mM EGTA, 10 mM HEPES, 2 mM ATP-Mg, and 1 mM cAMP, pH adjusted to 7.2 at room temperature (23–25°C) with CsOH. The tight-seal, whole-cell configuration of the patch-clamp technique (Hamill et al., 1981) was used on fluorescent green cells to record Ba^{2+} currents (I_{Ba}) through transiently-expressed Ca^{2+} channels.

Whole-cell currents were recorded using an Axopatch-1D amplifier (Axon Instruments Inc., Union City, CA), sampled at 10 kHz and

filtered at 2 kHz (−3 dB, four-pole Bessel filter; Axon Instruments), and acquired on-line by using the pClamp6 program (Axon Instruments). Pipette and cell capacitances were compensated in all experiments. Series resistance was also compensated in the range of 60 to 80%. Extracellular media were exchanged using a gravity-fed bath perfusion system (BPS-4; ALA Scientific Instruments, Westbury, NY). The flow rate was approximately 5×10^{-3} ml/s. The distance of the flow pipette from the cell was approximately 150 μm and the pipette tip diameter was 300 μm. All experiments were carried out at room temperature (23–25°C).

For all experiments, once the whole-cell configuration had been attained, current was allowed to stabilize for approximately 5 min before beginning recordings. Cells for which responses continued to decline after this time in the absence of treatments were not recorded further. Except when noted otherwise, a pulse protocol was used to examine the effects of Pb^{2+} on membrane currents. A hyperpolarizing pulse with one quarter of the test pulse magnitude was applied to measure the leak current, followed by a depolarizing pulse to elicit inward current. Linear components of leak and capacitive current were not subtracted from these records. Therefore, effects of Pb^{2+} on inward current, leak current, and capacitive current could be examined in consecutive traces. Leak subtraction was performed offline by subtracting the scaled current observed with the P/N protocol (Axon Instruments, 1994). In the absence of Pb^{2+}, current rundown over the duration of the recording session was approximately 10% (results not shown) irrespective of the phenotype of Ca^{2+} channel examined. The block of current by Pb^{2+} was estimated as inhibition of peak I_{Ba} during 150-ms test pulses from a holding potential of −70 to 0 mV (α_{1C}), −90 to + 20 mV (α_{1B}), and −90 to 0 mV (α_{1E}) at a frequency of 0.1 Hz until steady-state inhibition was reached. For concentration-response studies, increasing concentrations of Pb^{2+} were applied sequentially to a cell while stimulation of the cell was continued at 0.1 Hz. For these studies, a given concentration of Pb^{2+} was applied until the response reached a plateau; this typically occurred within 1 min of exposure to this concentration of Pb^{2+}.

Statistical Analysis. Origin (Origin Labs, Northampton, MA) and pClamp (Axon Instruments) software suites were used to perform linear and nonlinear fit of data. Statistical comparisons were analyzed using Student's t test or one-way analysis of variance. Results are expressed as mean ± S.E.M., and $p < 0.05$ was considered statistically significant.

Results

Concentration-Dependence of Effect of Pb^{2+}on I_{Ba}. Ca^{2+} channels transiently expressed in HEK 293 cells using a constant $\alpha_{2b}\delta$ and β_{3a} subunit yielded current characteristic of the α_1 subunit used in the experiment. These correspond to L-type using α_{1C}, N-type using α_{1B}, and R-type using α_{1E}. Current amplitudes for all three subtypes were voltage-dependent. No significant inward current was observed for L-type channels until the depolarizing step reached −30mV; it reached maximum amplitude at +10 mV and reversed sign at approximately +60 mV. The N-type current activated at approximately −10 mV and reached maximum amplitude at +10 mV, reversing sign at approximately +60 mV. R-type current began to activate at about −20 mV, reached maximum amplitude at 0 mV, and reversed sign at +50 mV. Current inactivation of R-type channels was faster based on inspection than for either L- or N-type channels.

The inward Ba^{2+} current (I_{Ba}) through all three channel subtypes was decreased in magnitude by 0.1 μM and 1.0 μM Pb^{2+}, but leak current and membrane capacitance were not changed (Fig. 1), indicating that the inhibitory effect of Pb^{2+} was not caused by disruption of membrane electrical properties. Comparison of the steady-state current traces obtained before and after application of 0.1 and 1.0 μM Pb^{2+} illustrates the differential sensitivity of the three channel subtypes at two different concentrations. Subsequently, a wider range of concentrations of Pb^{2+} was applied sequentially to determine the concentration-dependence of current reduction. Peak current amplitudes for each pulse were normalized to the values in the absence of Pb^{2+} and plotted against exposure time. The concentration-response curves were fitted using a sigmoidal function. Each step-wise increase in the concentration of Pb^{2+} caused a very rapid decline in peak current amplitude of all three Ca^{2+} channel subtypes (Fig. 2A). The concentration of Pb^{2+} that induced half-maximal current block (IC_{50}) after 2-min exposure was 0.38, 1.31, and

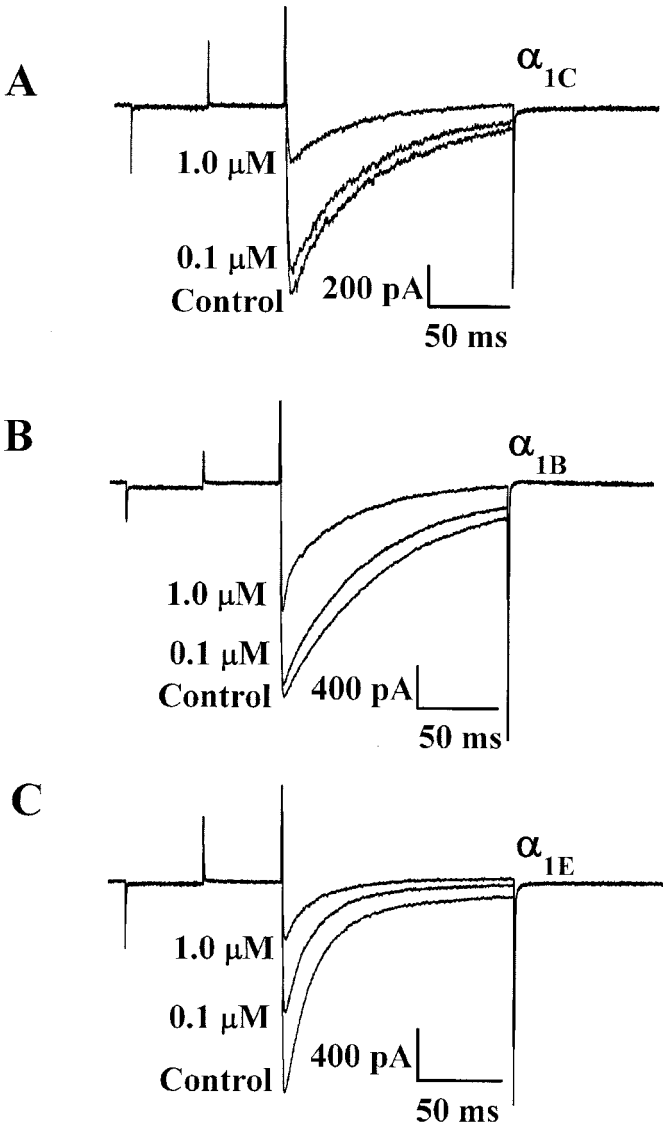

Fig. 1. Representative current traces showing effects of Pb^{2+} on A (α_{1C}), B (α_{1B}), and C (α_{1E}) types of voltage-activated Ca^{2+} channels transiently expressed in HEK 293 cells. One of the three classes of α_1 subunits (α_{1C}, α_{1B}, and α_{1E}) of human neuronal Ca^{2+} channels was expressed in HEK 293 cells together with $\alpha_{2b}\delta$ and β_{3a} subunits in each experiment. Whole-cell Ba^{2+} (20 mM Ba^{2+}) currents were evoked by 150-ms depolarizations from a holding potential of −70 mV (α_{1C}) or −90 mV (α_{1B} and α_{1E}) to a test potential of 0 mV (α_{1C} and α_{1E}) or +20 mV (α_{1B}). The effect of 0.1 μM and 1.0 μM Pb^{2+} on elicited currents is shown. Current responses were filtered at 2 kHz and leak current was not subtracted.

0.10 μM for L-, N-, and R-type currents, respectively (Fig. 2B). The putative R-type Ca^{2+} channel currents elicited by transfection with the α_{1E} subunit seemed to be more sensitive than the L- and N-types. Pb^{2+} also accelerated the inactivation time of all three subtypes of channels, but had no significant effect on activation kinetics (Fig. 1). This is seen more clearly in a comparison of normalized current traces described below.

Voltage-Dependence of Reduction of I_{Ba} by Pb^{2+} . To examine whether the decline of I_{Ba} caused by Pb^{2+} is voltage-dependent, we compared the current-voltage relationships in the presence or absence of Pb^{2+}. After a 2-min exposure to 0.1, 0.5, and 1 μM Pb^{2+} (concentrations approximating the IC_{50} values) for L-, N-, and R- Ca^{2+} channel subtype-expressing cells, respectively, Pb^{2+} reduced peak current amplitude at all potentials that elicited current but did not alter either the threshold of activation of I_{Ba} or the reversal potential. The potential at which maximum current was elicited was also not altered by Pb^{2+} for any of the channels. Inhibition of peak current by Pb^{2+} was similar at all voltage steps and there was little suggestion of any voltage-dependent reduction of peak current by Pb^{2+} (Fig. 3A). Conversion of the current-voltage curves to conductance-voltage curves by dividing the observed current by the driving force yielded the plots shown in Fig. 3B. Boltzmann fits to the data were used to calculate the voltage at which half the channels open ($V_{1/2}$). $V_{1/2}$ was -1.6 mV in control and -0.2 mV after 2-min exposure to 0.5 μM Pb^{2+} in L-type, $V_{1/2}$ = 1.5 and 1.4 mV before and after 2-min exposure to 1.0 μM Pb^{2+} in N-type, and $V_{1/2}$ = -10.3 and -11.0 mV before and after exposure of 0.1 μM Pb^{2+} in R-type channels. None of these differences were significant ($p > 0.05$).

Effects of Pb^{2+} on the onset of inactivation for the three types of currents suggest that Pb^{2+} might alter the steady-state availability of the three subtypes of Ca^{2+} channels. We used a conventional protocol to examine the voltage-dependence of inactivation using 8-s conditioning steps at potentials between -100 and 0 mV followed by a test step. As the conditioning potential was changed from -100 to 0 mV, an increasing proportion of channels became inactivated. The

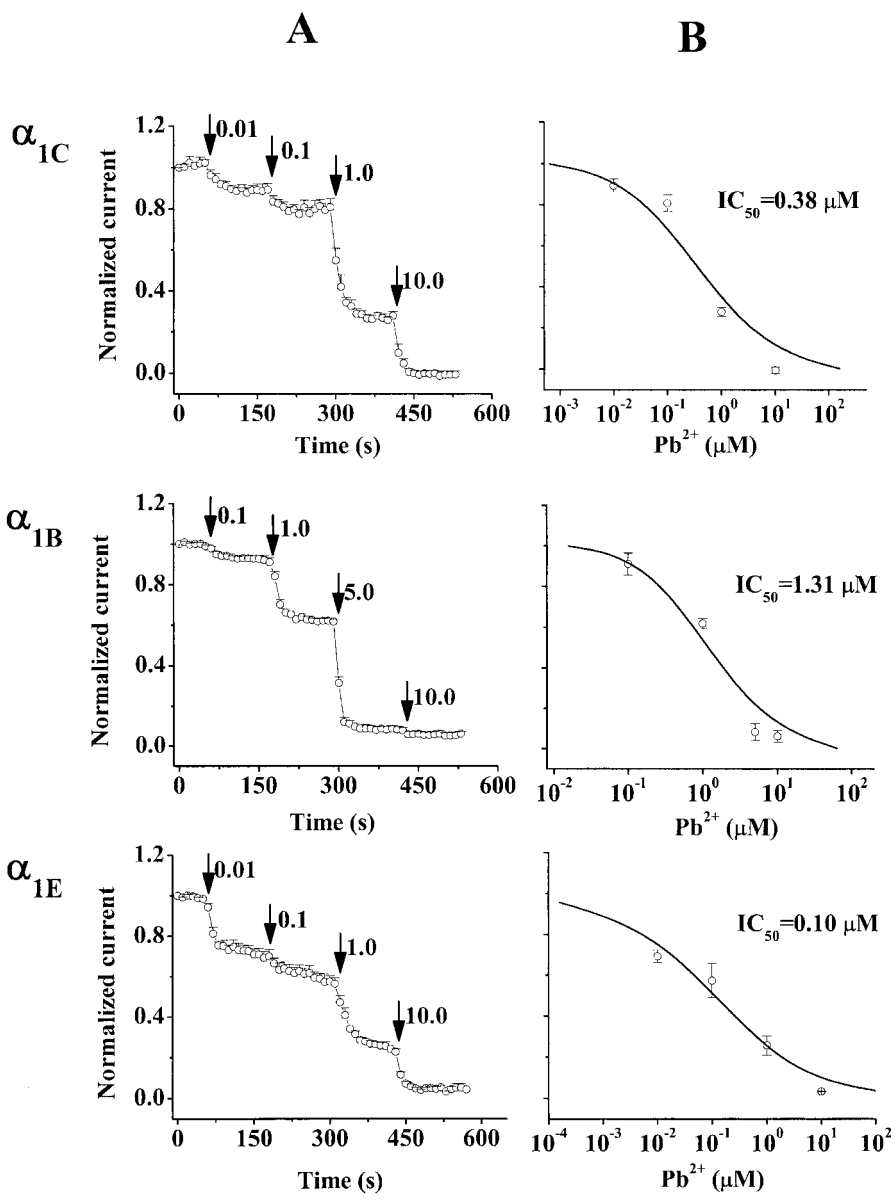

Fig. 2. Concentration-dependent inhibition of Pb^{2+} on I_{Ba} in HEK 293 cells expressing either α_{1C}, α_{1B}, or α_{1E} subunit of human neuronal Ca^{2+} channels together with the $\alpha_{2b}\delta$ and β_{3a} subunits. A, time course of block with different concentrations of Pb^{2+} on normalized peak current. B, amplitude of inward Ba^{2+} currents (20 mM Ba^{2+}) recorded before and after a 2-min exposure to different concentrations of Pb^{2+} were fitted using $I_{[Pb^{2+}]}/I_{Control} = [1+([Pb^{2+}]_e/IC_{50})^n]^{-1}$ with an IC_{50} = 0.38, 1.31, and 0.10 μM for α_{1C}, α_{1B}, and α_{1E}, respectively. Values shown are the mean ± SEM of seven to nine different cells. Cells expressing Ca^{2+} channels containing α_{1C}, α_{1B}, or α_{1E} subunit together with $\alpha_{2b}\delta$ and β_{3a} subunits were depolarized from -70 to 0 mV, -90 to $+20$ mV, or -90 to 0 mV, respectively, at a stimulation frequency of 0.1 Hz. Current responses were filtered at 2 kHz and leak current was subtracted.

voltage at which 50% of maximum inactivation occurred under our experimental conditions for L-, N-, and R-type channels was −44.4, −65.9, and −69.8 mV, respectively. The inactivation curve was shifted significantly to −72.2 mV (shift of about 6 mV) and −79.7 mV (shift of about 10 mV) for N- and R-types, respectively, in the presence of Pb^{2+}. However, there was no significant change in the inactivation curve for L-type channels (−44.4 versus −44.9 mV) before and after Pb^{2+}exposure (Fig. 4A).

To illustrate the voltage-dependence of Pb^{2+}-mediated current decline on inactivation curves, we plotted the percentage reduction of current calculated from the curves in Fig. 4A as a function of conditioning potentials (Fig. 4B). For all three channel subtypes, the percentage of current reduction by Pb^{2+} seemed to be voltage-dependent. At a membrane potential of −100 mV, 100% of the channels were estimated to be in the closed state, where the maximal percentage reduction was 32% (0.5 μM Pb^{2+}), 45% (1.0 μM Pb^{2+}), and 67% (0.1 μM Pb^{2+}) for L-, N-, and R-type channels, respectively. During the conditioning pulse, potentials changed from −100 to 0 mV and the current inhibition caused by Pb^{2+} gradually diminished (Fig. 4B), suggesting that Pb^{2+} has high affinity for the closed state. Comparison of voltage-dependent reduction of steady-state inactivation for all three subtypes of channels caused by Pb^{2+} concentrations approximating their respective IC_{50}, indicated further that R-type current was more sensitive to Pb^{2+} at more negative potentials than was L-or N-type current. This is consistent with their sensitivity to reduction of I_{Ba} by Pb^{2+} (IC_{50}) at resting potentials.

Reversibility of Reduction of I_{Ba} Caused by Pb^{2+}. Previous studies of native channels have shown that Pb^{2+}-induced reduction of I_{Ba} exhibited differential reversibility to wash with Pb^{2+}-free solution among different preparations (Audesirk and Audesirk, 1991; Reuveny and Narahashi, 1991; Hegg and Miletic, 1996). Therefore, we compared the reversibility of Pb^{2+}-induced reduction of I_{Ba} in HEK 293 cells expressing the three types of recombinant channels by washing the cells with Pb^{2+}-free solution for 3 min after 1-min exposure to 10 μM Pb^{2+}. In our hands, Pb^{2+}-free extracellular solution reversed 90, 92, and 71% of the Pb^{2+}-elicited block of current for L-, N-, and R-subtype–expressing cells, respectively (Fig. 5). Thus, the effects of Pb^{2+} on L- and N-type Ca^{2+} channels were almost completely reversible, whereas the Pb^{2+} block of R-type Ca^{2+} channels was incom-

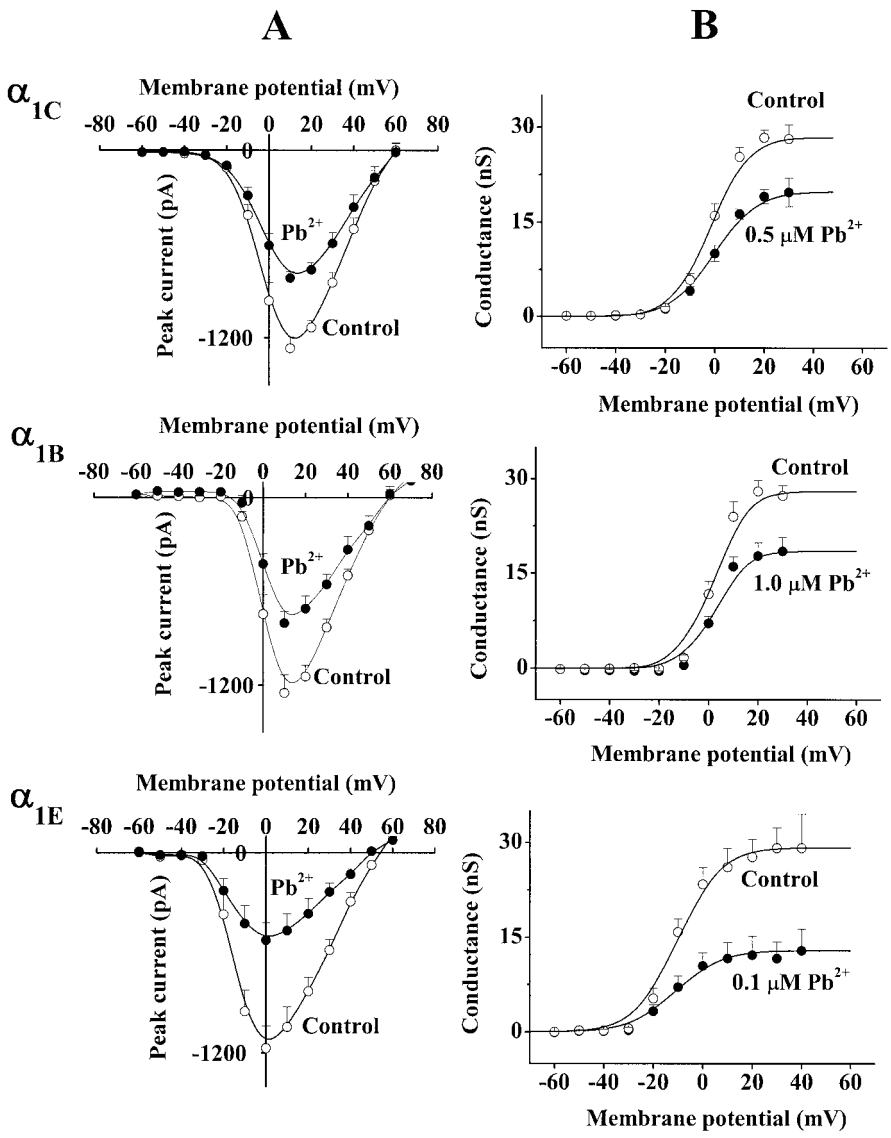

Fig. 3. Effect of Pb^{2+} on current-voltage relationship and conductance of I_{Ba} in HEK 293 cells expressing either α_{1C}, α_{1B}, or α_{1E} subunit together with $\alpha_{2b}\delta$ and β_{3a} subunits of human neuronal Ca^{2+} channels. A, current-voltage relationship of I_{Ba} (20 mM Ba^{2+}) recorded before and after 2-min exposure of 0.5, 1.0, and 0.1 μM Pb^{2+} for α_{1C}, α_{1B}, and α_{1E}, respectively. B, conductance-voltage curves were obtained from the current-voltage relationships in A. The conductance-voltage curves were fitted using the Boltzmann equation: $G(V) = G_{max}/(1+\exp[-(V - V_{1/2})/k])$, with control $V_{1/2}$ = −1.6 mV, k = 6.0 mV and, after 2-min 0.5 μM Pb^{2+} exposure, $V_{1/2}$ = −0.2 mV, k = 7.1 mV for α_{1C}; with control $V_{1/2}$ = 1.5 mV, k = 4.4 mV and, after 2-min 1.0 μM Pb^{2+} exposure, $V_{1/2}$ = 1.4 mV, k = 3.5 mV for α_{1B}; and with control $V_{1/2}$ = −10.3 mV, k = 6.9 mV and, after 2-min 0.1 μM Pb^{2+} exposure, $V_{1/2}$ = −11.0 mV, k = 7.7 mV for α_{1E}. Values shown are the mean ± S.E.M. of 4 to 14 different cells. Cells expressing Ca^{2+} channels containing α_{1C}, α_{1B}, or α_{1E} subunit were depolarized from −70 to 0 mV, −90 to +20 mV, or −90 to 0 mV, respectively. Current responses were filtered at 2 kHz and leak current was subtracted.

pletely reversible. α_{1E} encoded Ca^{2+} channels of human neuronal origin showed higher sensitivity and greater washout resistance after treatment with Pb^{2+} than did α_{1B} or α_{1C} encoded channels.

Concentration- and Voltage-Dependent Effects of Pb^{2+} on Inactivation Rate of I_{Ba}. Despite its strong reduction of peak current, Pb^{2+} seemed to accelerate the inactivation of I_{Ba} in cells expressing any of the three subtypes of Ca^{2+} channels. To explore this issue in greater detail, the concentration- and voltage-dependence of effects of Pb^{2+} on inactivation rate of I_{Ba} were examined. Figure 6A shows current through L-type channels in the absence or presence of three different concentrations of Pb^{2+}. The normalized current traces show that Pb^{2+} caused faster decay of L-type current in a concentration-dependent manner. To calculate the rate of current decay, we analyzed the portion of current that inactivated at 20 ms of depolarization (measured as [peak I_{Ba} − I_{20ms}]/peak I_{Ba}) and plotted it as a function of concentration of Pb^{2+} in Fig. 6B. The current decay rates varied in an almost linear fashion with increasing concentrations of Pb^{2+} ($r = 0.92$). A similar concentration-dependent effect was observed with N- and R-type Ca^{2+} channel-expressing cells (Figs. 7 and 8). In N-type Ca^{2+} channel-expressing cells, the current decay at 20 ms of depolarization was enhanced significantly from 25.0 ± 2.6% in control to 29.5 ± 2.7% with 0.1 μM Pb^{2+} ($p < 0.05$) and 45.8 ± 3.3% with 1.0 μM Pb^{2+} ($p < 0.05$) (Fig. 7B). In R-type Ca^{2+} channel-expressing cells, the current decay at 20 ms of depolarization was also increased from 48.5 ± 4.3% in control to 54.7 ± 4.6, 57.2 ± 4.5, and 55.9 ± 5.7% for 0.01, 0.1, and 1.0 μM Pb^{2+}, respectively.

We also examined the voltage-dependence of the effect of Pb^{2+} on current decay rate in all three subtypes of Ca^{2+} channels. Figure 9A compares currents through L-type channels recorded in the absence or presence of 0.5 μM Pb^{2+} at different membrane potentials. At each voltage tested, the normalized current traces show that 0.5 μM Pb^{2+} caused faster decay of L-type current depending on the command potential. In controls, the current decay at 20 ms of depolarization at different membrane potentials showed voltage-dependence ($p < 0.05$). After exposure to Pb^{2+}, the current decay at 20 ms of depolarization was increased significantly at membrane potentials of +10 to +40 mV, but not at −10 mV, 0 mV, and + 50 mV, indicating that the rate of current decay by Pb^{2+} in L-type channels is also voltage-dependent. Similarly, Pb^{2+}-induced current decay in N- and R-type

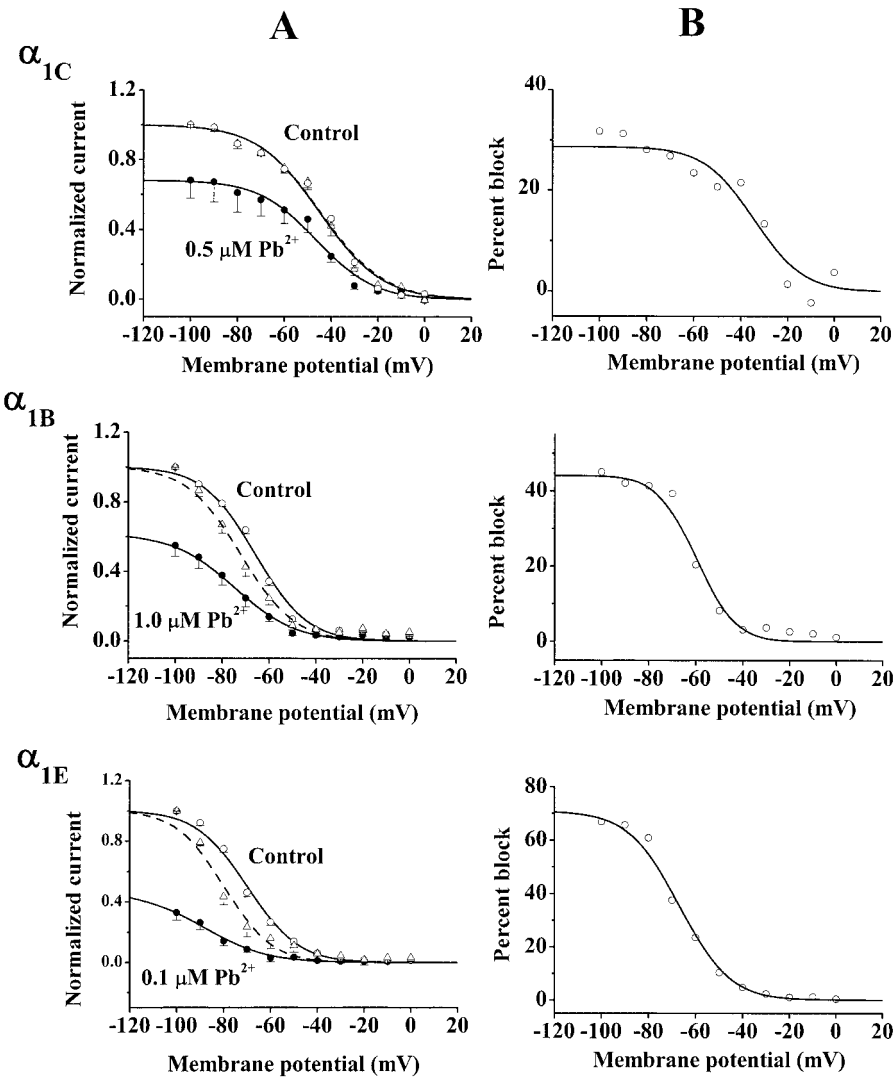

Fig. 4. Effect of Pb^{2+} on voltage-dependence of steady-state of inactivation curves of I_{Ba} currents (20 mM Ba^{2+}) in HEK 293 cells expressing human neuronal α_{1C}, α_{1B}, or α_{1E} subunit mediated L-, N-, or R-type Ca^{2+} channels, respectively. A, the normalized peak currents plotted versus the voltage of an 8-s conditioning prepulse during a 480-ms test pulse used to depolarize transfected cells from −70 to 0 mV, −90 to +20 mV, or −90 to 0 mV for α_{1C}, α_{1B}, or α_{1E} subunit-expressing cells, respectively. The peak currents before (control, ○) and after 3-min exposure of Pb^{2+} (●) were normalized using the largest current from control recorded after conditioning prepulses from −100 to 0 mV. The dashed lines (△) showing the peak currents after 3-min exposure of Pb^{2+} were normalized using the largest current from the same group within conditioning prepulses. The smooth curve is a Boltzmann function, $I/I_{max} = [1 + \exp\{(V - V_{1/2})/k\}]^{-1}$, with control $V_{1/2} = -44.4$ mV, k = 12.4 mV, and after 3-min 0.5 μM Pb^{2+} exposure, $V_{1/2} = -45.0$ mV, k = 12.1 mV for α_{1C}; with control $V_{1/2} = -65.9$ mV, k = 9.6 mV, and after 3-min 1.0 μM Pb^{2+} exposure, $V_{1/2} = -72.2$ mV, k = 10.0 mV for α_{1B} ($p < 0.05$), and with control $V_{1/2} = -69.8$ mV, k = 9.5 mV, and after 3-min 0.1 μM Pb^{2+} exposure, $V_{1/2} = -79.7$ mV, k = 8.2 mV for α_{1E} ($p < 0.05$). Values shown are the mean ± S.E.M. of five to seven different cells. Current responses were filtered at 2 kHz and leak current was subtracted. B, the percentage of block by Pb^{2+} over the range of voltages calculated from A. Block by Pb^{2+} was voltage-dependent.

channels was also voltage-dependent. In controls, the current decay at 20 ms of depolarization was voltage-dependent in N-type channels ($p < 0.05$; Fig. 10B) but not in R-type channels ($p > 0.05$, Fig. 11B). With Pb^{2+} exposure, the rate of current decay at 20 ms of depolarization was significantly different from 0 to +40 mV of tested membrane potentials for α_{1B} channels and from −10 to +40 mV for α_{1E} channels compared with respective controls.

Kinetics of Pb^{2+}-Induced Inactivation of I_{Ba}. The inactivation time constants were estimated by fitting the I_{Ba} decay to a biexponential function. In controls, the I_{Ba} kinetics at 10 mV in L-type channels exhibited a biexponential distribution; however, the N- and R-type currents showed single exponential distribution. In the presence of Pb^{2+}, the fast and slow components in I_{Ba} of L-type current were accelerated slightly but nonsignificantly from $\tau_{fast,\ control} = 16.2 \pm 2.0$ ms to $\tau_{fast,\ Pb} = 12.2 \pm 2.2$ ms, and from $\tau_{slow,\ control} = 72.5 \pm 14.3$ ms to $\tau_{slow,\ Pb} = 53.6 \pm 6.9$ ms with 0.5 μM Pb^{2+} ($p > 0.05$; Fig. 12A). At 1.0 μM, Pb^{2+} modulated the N-type current with a biexponential distribution; the transient fast component in the current decay was induced with $\tau_{fast,\ Pb} =$ 13.0 ± 2.9 ms and the slower inactivation time constant of the I_{Ba} was not significantly affected by Pb^{2+} (Fig. 12B). In R-type channels, I_{Ba} inactivation ensued with a fast time constant of 28.6 ± 2.2 ms and absence of intrinsic slow inactivation. Pb^{2+} significantly accelerated the decay time constant to 21.9 ± 1.6 ms ($p < 0.05$, Fig. 12C).

Discussion

The present study using transient expression from cDNA clones of specific subtypes of human neuronal Ca^{2+} channels was designed to characterize and compare the effects of Pb^{2+} on distinct subtypes of Ca^{2+} channels in isolation. Currently, there is only one previous report on the effects of Pb^{2+} on Ca^{2+} channels in isolation, addressing rabbit cardiac L-type Ca^{2+} channels stably expressed in HEK 293 cells (Bernal et al., 1997). Our results support several aspects of previous studies done on corresponding native channels and extends them using a system transiently expressing only one kind of channel in cells in which they are not normally expressed and in which only the pore-forming element of the channel varied.

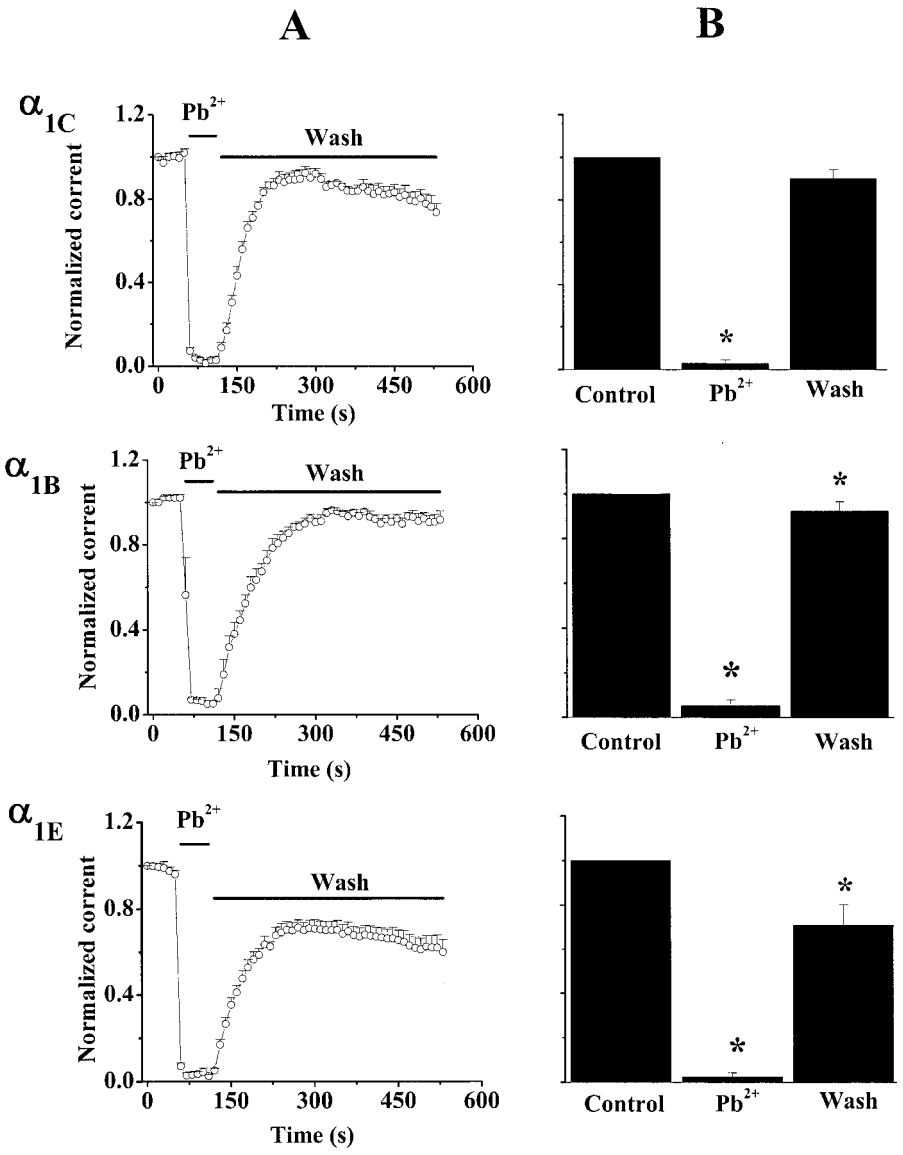

Fig. 5. Reversible reduction of peak Ba^{2+} current (20 mM Ba^{2+}) by 10 μM Pb^{2+} in HEK 293 cells expressing human neuronal α_{1C}, α_{1B}, or α_{1E} subunit mediated L-, N-, or R-type Ca^{2+} channels, respectively. A, peak current was rapidly blocked by 10 μM Pb^{2+} during 1-min exposure; washing with Pb^{2+}-free extracellular solution reversed the reduction of current caused by Pb^{2+} in all three subtypes. B, amplitude of I_{Ba} recorded before and after 1-min exposure to Pb^{2+} and after 3-min washing. Values shown are the mean ± S.E.M. of four to six different cells. *, significantly different from control. The value in the presence of 10.0 μM Pb^{2+} was significantly different for α_{1C}, α_{1B}, and α_{1E} ($p < 0.05$) compared with respective subtypes in control; the value after 3-min of wash was not significantly different for α_{1C} ($p > 0.05$), but was significantly different for α_{1B} ($p < 0.05$) and α_{1E} ($p < 0.05$). Cells expressing Ca^{2+} channels containing α_{1C}, α_{1B} or α_{1E} subunit were depolarized from −70 to 0 mV, −90 to +20 mV, or −90 to 0 mV, respectively, at a stimulation frequency of 0.1 Hz. Current responses were filtered at 2 kHz and leak current was subtracted.

We demonstrate here that: 1) Pb^{2+} is a reversible and potent inhibitor of currents expressed by cloned human neuronal α_{1C}, α_{1B}, and α_{1E} subunit-containing L-, N-, or R-type Ca^{2+} channels, respectively, expressed in HEK 293 cells. This Pb^{2+}-induced inhibition is effective at micromolar or submicromolar concentrations in a concentration-dependent manner, but the potency of Pb^{2+} for various Ca^{2+} channel phenotypes varies considerably. 2) The inactivation kinetics of the three types of channels studied is affected differently by Pb^{2+}. 3) Block by Pb^{2+} of α_{1B}- and α_{1C}- containing channels is more easily reversed than those of α_{1E} -containing channels.

In our hands, cloned human L-, N-, and R-type channels showed current characteristics and pharmacology essentially similar to native channels of the corresponding types in mammalian cells. The reduction of current amplitudes and reversibility of block by Pb^{2+} in our studies illustrate some differences among these three channel subtypes. These differences are summarized in tabular form in Table 1. The current from α_{1E} subunit-containing channel (R-type) is more sensitive to Pb^{2+} than are those from α_{1C} (L-type) or α_{1B} (N-type) channel-expressing cells. The peak current inhibition caused by Pb^{2+} was almost completely reversed for L- and N-type current (90 and 92%) but only incompletely for

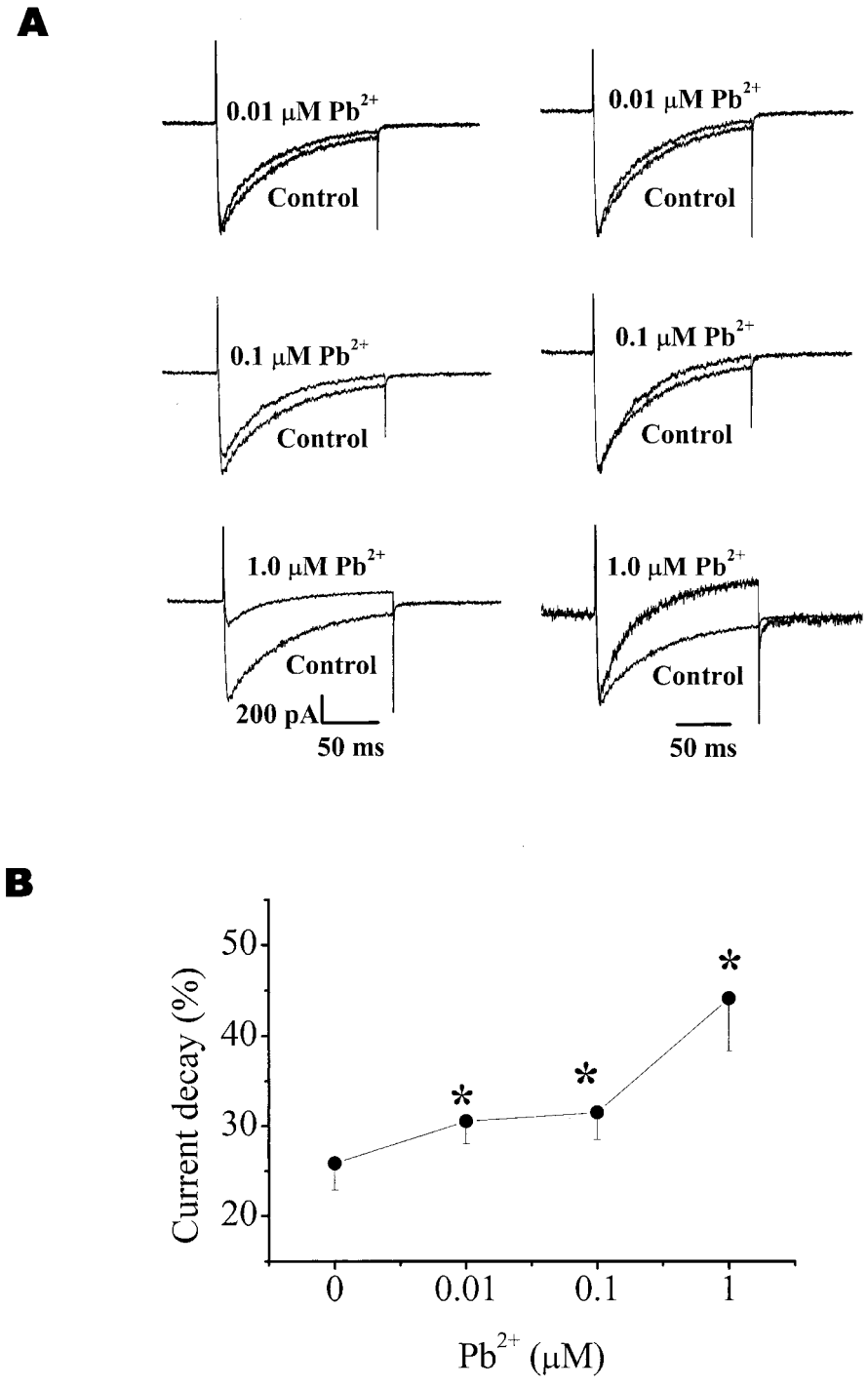

Fig. 6. Concentration-dependent effect of Pb^{2+} on decay rate of Ba^{2+} current (20 mM Ba^{2+}) in HEK 293 cells expressing human neuronal α_{1C} subunit mediated L-type Ca^{2+} channels. A, representative traces on the left showing original raw currents through α_{1C} channels elicited by depolarization from a holding potential of −70 to 0 mV in control and during exposure to three different concentrations of Pb^{2+}. The current traces normalized to peak current amplitudes are shown in the traces on the right. The rate of current decay during exposure to Pb^{2+} exhibited concentration-dependence. B, the percentage current decay at 20 ms of depolarization was plotted as a function of concentrations of Pb^{2+}. Values shown are the mean ± S.E.M. of nine different cells. Pulse steps (150 ms) from −70 to 0 mV were used to examine the decay phase and current responses were filtered at 2 kHz. As shown by the asterisks (*), the current decay in presence of Pb^{2+} was significantly different from the control value at 0.01, 0.1 Pb^{2+}, and 1.0 μM Pb^{2+} ($p < 0.05$).

R-type current (71%) by washing with Pb^{2+}-free solution. The potency of Pb^{2+} as a blocker is quite high; in the presence of 20 mM Ba^{2+} as charge carrier, for both R- and L-type currents, the apparent IC_{50} values were less than 1 μM total added Pb^{2+}. Furthermore, inhibition occurs very rapidly and at least for α_{1B} and α_{1C} readily reaches a plateau. For α_{1E} current amplitude also declines rapidly in the presence of Pb^{2+} but does not reach an apparent plateau as readily, suggesting that perhaps a slower continuing inhibitory action is occurring. This effect is reminiscent of the actions of neurotoxic mercurials on cloned, heterologously expressed Ca^{2+} channels (Peng et al., 2001, 2002). The current-voltage relationships for all three of these types of Ca^{2+} channels were unaffected by exposure to Pb^{2+}. However, the steady-state inactivation relationships were shifted to more negative potentials after exposure to Pb^{2+} for N- and R-type, but not L-type currents. Pb^{2+} accelerated the inactivation rate of current in all three subtypes of Ca^{2+} channels in a concentration- and voltage-dependent manner. Therefore, it seems that Pb^{2+} has high affinity for Ca^{2+} channels in the closed state.

In the present study, we found both similarities and differences in the blocking ability of Pb^{2+} compared with native currents from previous studies. In rat dorsal root ganglion neurons, the component of whole-cell current ascribed to N-type channels, based on its sensitivity to ω-conotoxin GVIA (IC_{50} = 1.0 μM), is slightly more sensitive than is L-type current (IC_{50} = 6.0 μM) (Evans et al., 1991). In N1E-115 neuroblastoma cells, which possess both L- and T-type Ca^{2+} channels, Pb^{2+} inhibited L-type Ca^{2+} channels with an IC_{50} of 0.7 μM and T-type with an IC_{50} of 1.3 μM (Audesirk and Audesirk, 1991). In rat hippocampal neurons, Pb^{2+} is some-

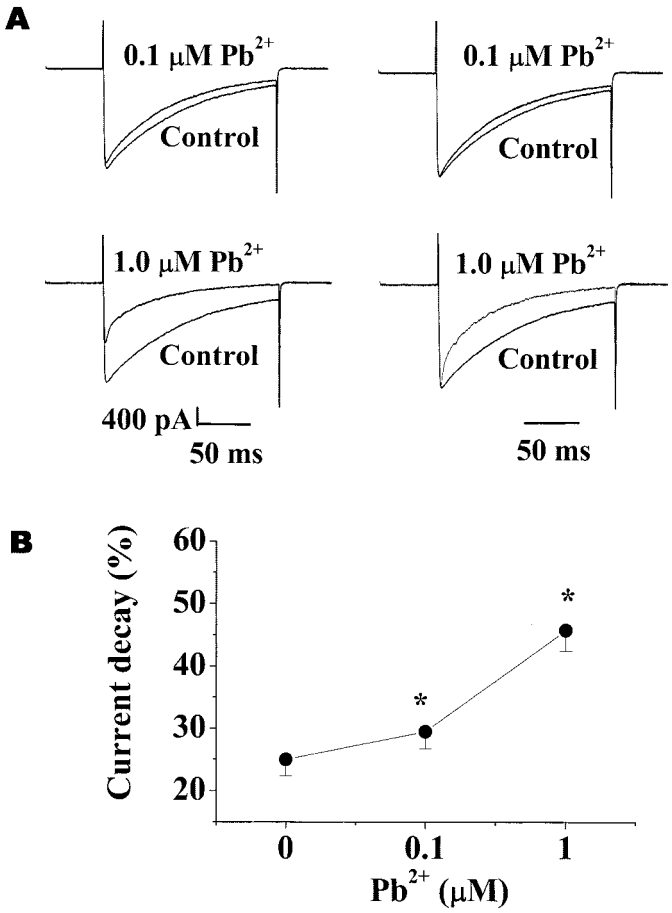

Fig. 7. Concentration-dependent effect of Pb^{2+} on decay rate of I_{Ba} (20 mM Ba^{2+}) in HEK 293 cells expressing human neuronal α_{1B} subunit-mediated N-type Ca^{2+} channels. A, representative traces on the left showing original currents through α_{1B} channels elicited by depolarization from a holding potential of −90 to +20 mV in control and in the presence of 0.1 and 1.0 μM Pb^{2+}. The current traces normalized to peak current amplitudes are shown on the right. The rate of current decay during exposure to Pb^{2+} exhibited concentration-dependence. B, the percentage decay at 20 ms of depolarization was plotted as a function of concentrations of Pb^{2+}. Values of the mean ± S.E.M. are from six different cells in which 150-ms pulse steps were used to examine the decay phase and current responses were filtered at 2 kHz. *, current decay in the presence of Pb^{2+} was significantly different from the control value at both concentrations of 0.1 and 1.0 μM Pb^{2+} ($p < 0.05$).

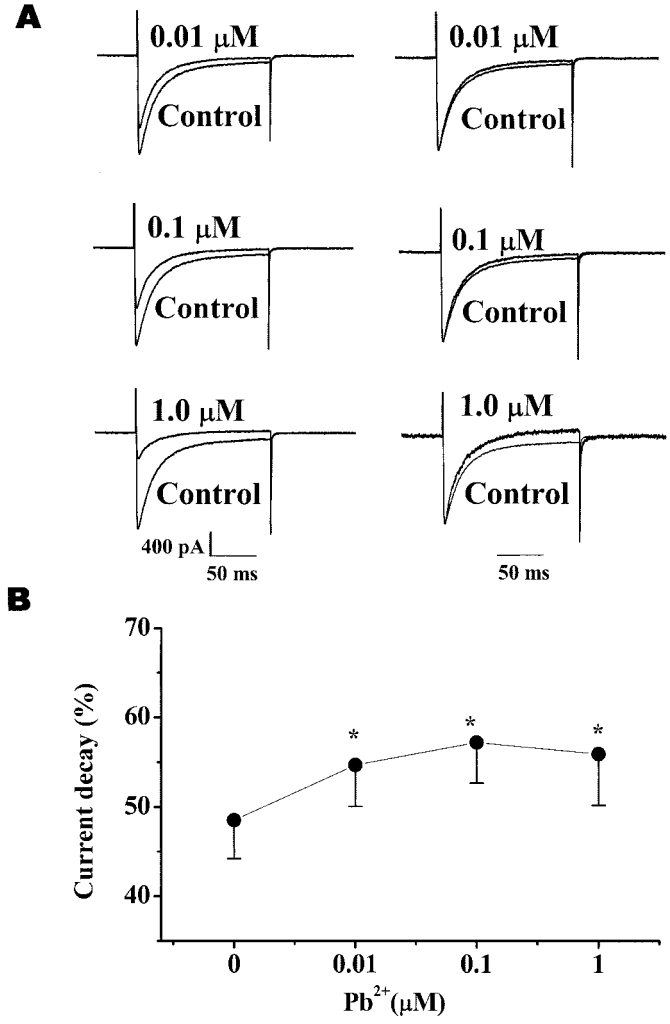

Fig. 8. Concentration-dependent effect of Pb^{2+} on decay rate of Ba^{2+} current (20 mM Ba^{2+}) in HEK 293 cells expressing human neuronal α_{1E} subunit mediated R-type Ca^{2+} channels. A, representative traces on the left showing original currents through α_{1E} channels elicited by depolarization from a holding potential of −90 to 0 mV in control and in presence of different concentrations of Pb^{2+}. The currents normalized to peak current amplitudes are shown on the right. The rate of current decay during exposure to Pb^{2+} exhibits concentration-dependence. B, the percentage decay at 20 ms of depolarization was plotted as a function of Pb^{2+} concentration. Values of the mean ± S.E.M. are from five different cells in which 150-ms pulse steps were used to examine the decay phase; current responses were filtered at 2 kHz. *, current decay in the presence of Pb^{2+} were significantly different from the control value at 0.01, 0.1, and 1.0 μM Pb^{2+} ($p < 0.05$).

what more selective against presumptive L-type channels than N-type channels (Audesirk and Audesirk, 1993). On the basis of IC_{50} values, our results demonstrate that α_{1E} current (R-type) was most sensitive to Pb^{2+}, followed by α_{1C} current (L-type) and then α_{1B} current (N-type). This suggests that differential susceptibility to Pb^{2+} by different types of Ca^{2+} channels occurs even when the various channels are expressed in the same cell type. The differences between our results and previously reported native channel studies could also be due in part to our using the same $\alpha_2\delta$ and β subunit with all three α_1 subunits.

Washing with Pb^{2+}-free solution reversed the block of I_{Ba} of all three types of Ca^{2+} currents. However, the extent of reversibility of I_{Ba} in the three subtypes varied. Pb^{2+}-induced block of L- and N-type Ca^{2+} channels was more easily reversed than for R-type Ca^{2+} channels. Previous studies have reported both reversible and irreversible Ca^{2+} channel current inhibition by Pb^{2+} in different preparations. In both rat hippocampal neurons (Audesirk and Audesirk, 1993) and N1E-115 cells (Audesirk and Audesirk, 1991; Oortgiesen et al., 1993), inhibition of current flow through Ca^{2+} channels by Pb^{2+} was generally completely reversible. In rat dorsal root ganglion neurons, on the other hand, the effect of Pb^{2+} was only partially reversible (Büsselberg et al., 1994). However, the block of Ca^{2+} current by Pb^{2+} in PC12 cells was irreversible (Hegg and Miletic, 1996). The concentration-independent and washout-resistant block in rat dorsal root ganglion and snail neurons was termed 'irreversible inhibition' by Audesirk (1993). In another study, full recovery from Pb^{2+} block of rabbit cloned cardiac L-type Ca^{2+} channel

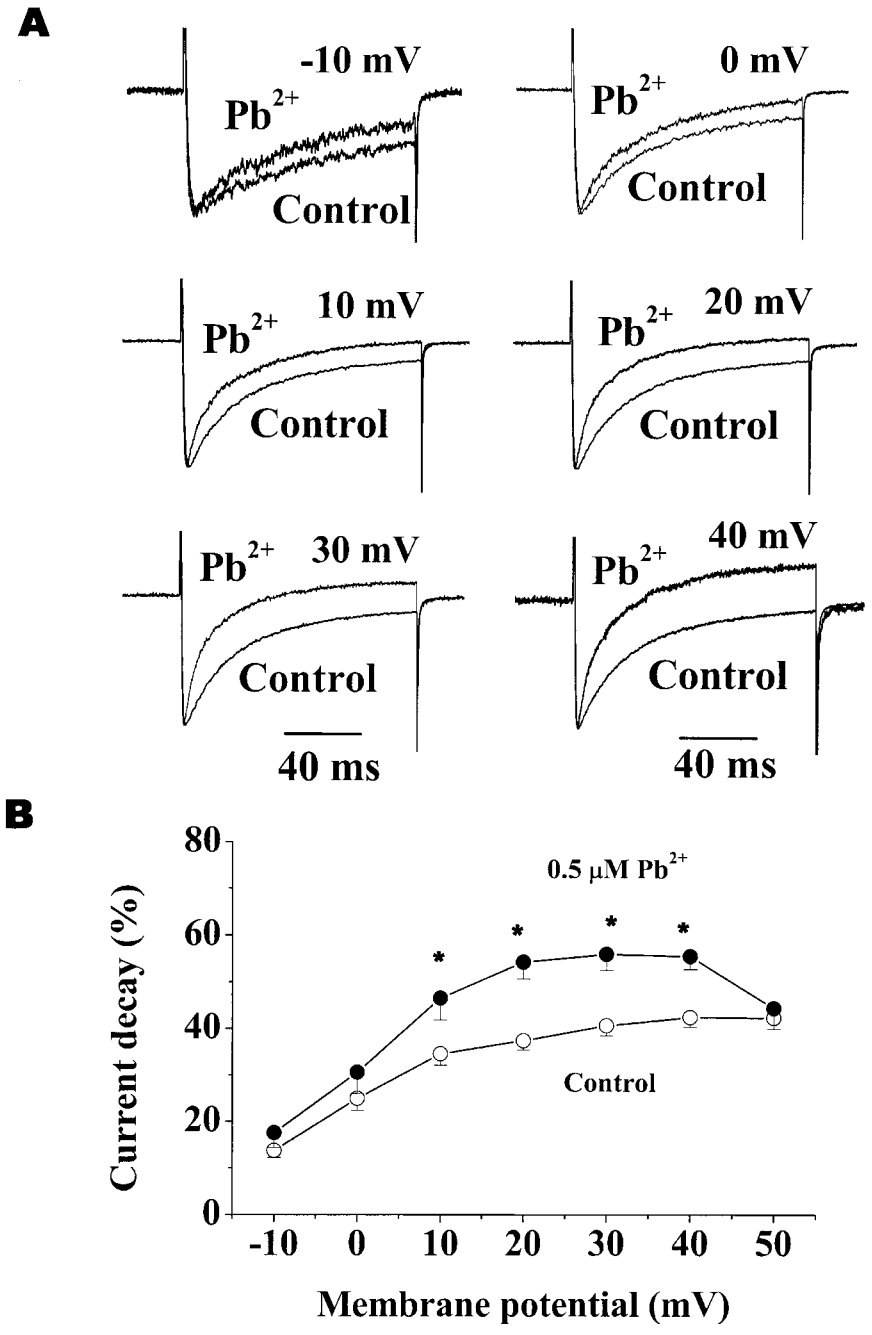

Fig. 9. Voltage-dependent effect of Pb^{2+} on decay rate of Ba^{2+} current (20 mM Ba^{2+}) in HEK 293 cells expressing human neuronal α_{1C} subunit-mediated L-type Ca^{2+} channels. A, representative traces showing effect of 0.5 μM Pb^{2+} on Ba^{2+} current at different membrane potentials. Currents, shown normalized to maximum current amplitude, were elicited by depolarization from a holding potential of -70 mV to different membrane potentials in the absence (control) and presence of 0.5 μM Pb^{2+}. The rate of current decay by Pb^{2+} at different membrane potentials exhibited voltage-dependence. B, the current decay at 20 ms of depolarization as percentages was plotted as a function of membrane potentials. Values shown are the mean ± S.E.M. of five to eight different cells. Pulse steps (150 ms) were used to examine the decay phase and current responses were filtered at 2 kHz. *, current decay in the presence of 0.5 μM Pb^{2+} was significantly different at 10, 20, 30, and 40 mV ($p < 0.05$) of membrane potential compared with the respective membrane potential in control.

currents expressed in HEK 293 cells required treatment with heavy metal chelators such as meso-2,3-dimercaptosuccinic acid, 2,3-dimercapto-1-propanesulfonic acid, and EDTA (Bernal et al., 1997). In our hands, simple washout almost completely reversed Pb^{2+} block of L- and N-type currents (more than 90% of control); however, R-type current showed some resistance to simple washout. Examining the IC_{50} values, it seems that α_{1E} subtype-expressing channels may have higher affinity for Pb^{2+} than do α_{1C} and α_{1B} subunit-expressing channels. Two sets of divalent cation binding sites created by four negatively charged glutamate residues, one between each SS1-SS2 pore-lining segment of the four repeated domains, are believed to be present in the pore of Ca^{2+} channels (Parent and Gopalakrishnan, 1995). Thus, the more reversible component of block may represent Pb^{2+} binding to the more externally located lower affinity sites; the washout-resistant block may be attributable to Pb^{2+} binding to the second, more internally located site, from which it dissociates only slowly (Bernal et al., 1997).

The mechanism by which Pb^{2+} blocks voltage-activated Ca^{2+} channel is poorly understood. If Pb^{2+} binds to a site within the channel, the blocking effect should be voltage-dependent as predicted by a simple model of voltage-dependent channel blockade (Woodhull, 1973). In our experiments, Pb^{2+} did not change the voltage at which the maximal current is elicited, which would indicate that there is no change in kinetics of channel activation. Therefore, Pb^{2+} binding may reduce the number of available functional channels, causing reduction in current amplitude rather than changes in the properties of channels through which current is carried. Our results are consistent with those for native channels in rat dorsal root ganglion cells (Büsselberg et al., 1994), N1E-115 neuroblastoma cells (Audesirk and Audesirk, 1991) and rat hippocampal neurons (Audesirk and Audesirk, 1993). However, they are at divergence with another report, in which Pb^{2+} block caused the voltage at which peak current is generated to shift in the hyperpolarizing direction (Büssel-

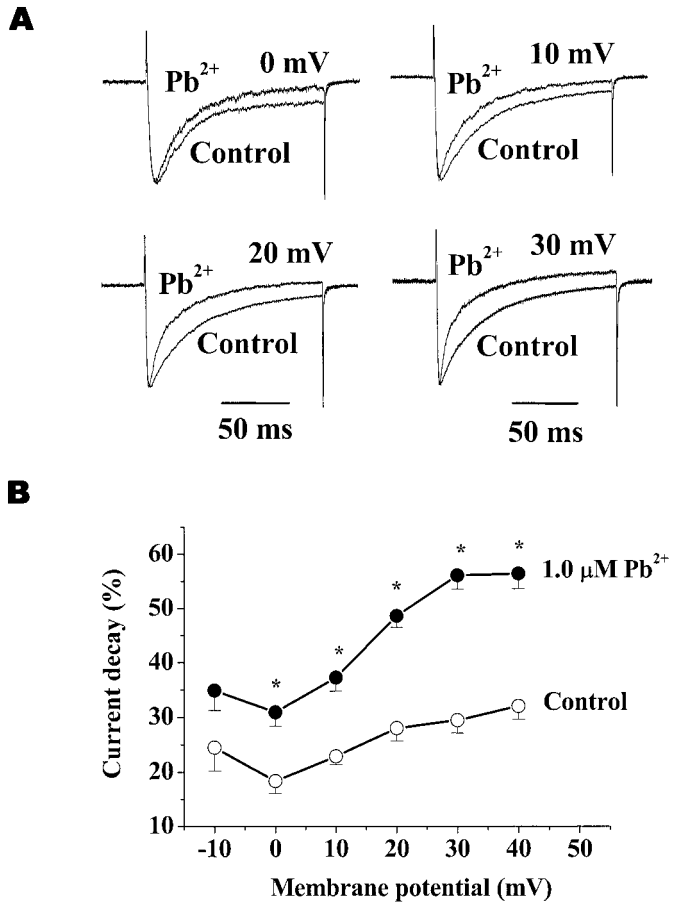

Fig. 10. Voltage-dependent effect of Pb^{2+} on decay rate of Ba^{2+} current (20 mM Ba^{2+}) in HEK 293 cells expressing human neuronal α_{1B} subunit mediated N-type Ca^{2+} channels. A, representative traces showing effect of 1.0 μM Pb^{2+} on Ba^{2+} current at different membrane potentials. Currents, shown normalized to maximum current amplitude, were elicited by depolarization from a holding potential of −90 mV to different membrane potentials in the absence and presence of 1.0 μM Pb^{2+}. The rate of current decay by Pb^{2+} at different membrane potentials exhibited voltage-dependence. B, the percentage rate of current decay at 20 ms of depolarization as percentages was plotted as a function of membrane potential. Values shown are the mean ± S.E.M. of six different cells. Pulse steps (150 ms) were used to examine the decay phase and current responses were filtered at 2 kHz. *, current decay in the presence of 1.0 μM Pb^{2+} was significantly different at 0 to 40 mV of membrane potential compared with the respective membrane potential in control Pb^{2+}-free ($p < 0.05$).

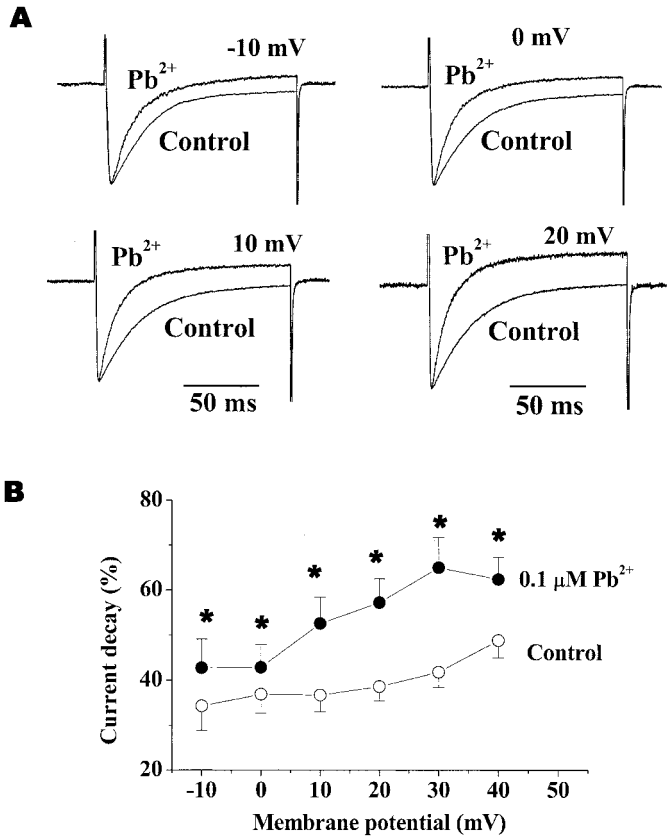

Fig. 11. Voltage-dependent effect of Pb^{2+} on decay rate of Ba^{2+} current (20 mM Ba^{2+}) in HEK 293 cells expressing human neuronal α_{1E} subunit mediated R-type Ca^{2+} channels. A, representative traces showing effect of 0.1 μM Pb^{2+} on Ba^{2+} current at different membrane potentials. Currents, shown normalized to maximum current amplitude, were elicited by depolarization from a holding potential of −90 mV to different membrane potentials in the absence and presence of 0.1 μM Pb^{2+}. The current decay rates by Pb^{2+} at different membrane potentials exhibited voltage-dependence. B, the rate of current decay at 20 ms of depolarization as percentages was plotted as a function of membrane potentials. Values shown are the mean ± S.E.M. of six different cells. Pulse steps (150 ms) were used to examine the decay phase and current responses were filtered at 2 kHz. *, decay value in the presence of 0.1 μM Pb^{2+} was significantly different at −10, 0, 10, 20, 30, and 40 mV ($p < 0.05$) of membrane potential compared with the respective membrane potential in control.

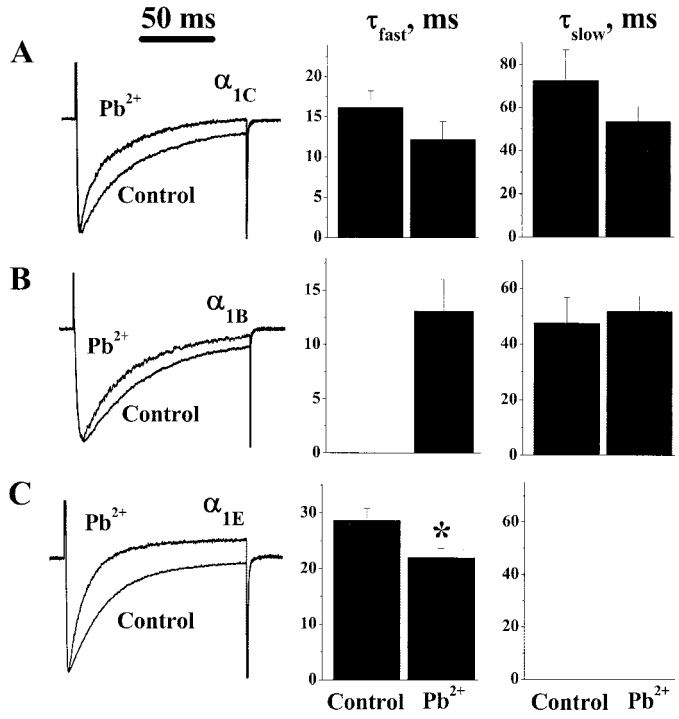

Fig. 12. Pb^{2+}-induced modulation of current Ba^{2+} current (20 mM Ba^{2+}) decay in HEK 293 cells expressing human neuronal α_{1C} (A), α_{1B} (B), or α_{1E} (C) subunit mediated L-, N-, or R-type Ca^{2+} channels, respectively. Representative traces showing inward currents through the indicated channels during 150-ms depolarization from holding potential of −70 mV (α_{1C}) or −90 mV (α_{1B} and α_{1E}) to 0 mV (α_{1C} and α_{1E}) or +20 mV (α_{1B}) in control and in the presence of Pb^{2+} (0.5 μM for α_{1C}, 1.0 μM for α_{1B}, and 0.1 μM for α_{1E}) (left). The time constants of fast (τ_{fast}, middle) and slow (τ_{slow}, right) in control and in the presence of Pb^{2+} were estimated by fitting biexponential functions to the current traces. Values of the mean ± S.E.M. are from five to six different cells. The current responses were filtered at 2 kHz and leak current was subtracted. Relatively speaking, no fast component in inactivation for α_{1B} and no slow component in inactivation for α_{1E} was observed. *, decay time constant in the presence of Pb^{2+} was significantly different from the control value for α_{1E} ($p < 0.05$).

berg et al., 1991). Our studies suggest that Pb^{2+}-induced block of Ca^{2+} currents may be independent of channel opening and may not necessarily require open channels.

We can also discount Pb^{2+} interacting with membrane surface charges or with other specific high-affinity sites to alter charge screening because actions at these sites have been reported to shift the current-voltage curve and activation curve to more depolarizing potentials (Byerly et al., 1985). Absence of a shift in the current-voltage relationship curves in our studies rules this out as a likely mechanism of Pb^{2+} block of Ca^{2+} channels. Unlike the above, Pb^{2+} induced the steady-state inactivation curves to shift to more negative potentials in N- and R-type channels but not L-type channels. The potency of block was enhanced greatly at hyperpolarizing potentials that promote the channel being in the resting state. At more negative potentials, Pb^{2+} block for the three subtypes of Ca^{2+} channels in our study shows greater potency than that at positive potentials (Fig. 4). These observations suggest that Pb^{2+} has greater affinity for closed channels than for the inactivated state. This is consistent with previous reports in PC12 cells, in which block of I_{Ca} by Pb^{2+} has been reported to be associated with the closed state of channels (Shafer, 1998).

TABLE 1

Comparative effects of Pb^{2+} on various parameters in different recombinant Ca^{2+} channel subtypes

$\alpha_{2\delta}$ and β subunits were used for all studies. 20 mM Ba^{2+} was the charge carrier. Pb^{2+} was applied extracellularly by continuous bath superfusion. Reversibility was tested using a 3-min wash with Pb^{2+}-free physiological saline after 1-min exposure to a concentration that approximated the relative IC_{50} for that channel subtype.

	α_{1C}	α_{1B}	α_{1E}
IC_{50} (μM)	0.38	1.31	0.10
Activation curve	No effect	No effect	No effect
Inactivation curve	No effect	Negative shift	Negative shift
Reversibility	>90%	>90%	~70%
Inactivation	Increase	Increase	Increase

Inactivation is an important aspect of Ca^{2+} channel gating, which controls the amount of Ca^{2+} entry during an action potential, and plays an important role in tissue-specific Ca^{2+} signaling. Inactivation kinetics of Ca^{2+} channels are determined by the intrinsic properties of their pore-forming α_1-subunits and by interactions with other channel subunits (Hering et al., 2000). The inactivation of Ca^{2+} channels may involve internal or external conformational changes as well as responses to elevation of intracellular [Ca^{2+}]. In our study, Pb^{2+} accelerated the inactivation rate of current in all three subtypes of Ca^{2+} channels in a concentration- and voltage-dependent manner, suggesting that Pb^{2+} might modulate the binding site associated with fast inactivation and increase the rate of entry into inactivated states or slow the recovery to resting state. External Pb^{2+} affected the inactivation rate over a range of concentrations that produced substantial block of peak current. Therefore, Pb^{2+} might speed the rate of entry of channels into the inactivated state. This inactivated state can be reached from the open state by inactivation followed by binding, or binding followed by inactivation. Because Pb^{2+} had higher potency at hyperpolarizing potentials than at depolarizing potentials, Pb^{2+} binding with high affinity apparently precedes inactivation and prevents recovery.

Conformational change has been suggested in C-type inactivation of K^+ channels with extracellular Cd^{2+}, tetraethylammonium, and sulfhydryl modifiers (Hoshi et al., 1990; Choi et al., 1991; Lopez-Barneo et al., 1993; Yellen et al., 1994; Baukrowitz and Yellen, 1995; Liu et al., 1996). The kinetics of block by Pb^{2+} of voltage-dependent Ca^{2+} channels in our study supports the possibility that Pb^{2+} may be causing a conformational change in channels resulting in fast inactivation. The Pb^{2+}-induced shift of steady-state inactivation is consistent with the inactivation rate of current as demonstrated in Fig. 12. At 20 mV, Pb^{2+} accelerated the fast-inactivation of all three subtypes of channels. This Pb^{2+}-induced inactivation state at least partially reflects Pb^{2+}-induced transitions of open channels to an inactivated state. Pb^{2+}-induced conformational change near the external mouth of the Ca^{2+} channel pore would rapidly facilitate the inactivation time course of currents in all three subtypes of Ca^{2+} channels.

In summary, Pb^{2+} is a potent and generally reversible inhibitor of human neuronal L-, N-, and R-type Ca^{2+} channels expressed in HEK 293 cells. It seems likely that Pb^{2+} blocks Ca^{2+} current by acting at a site external to the channel, where it competes with Ca^{2+}, impeding its entry, but the binding to this is not voltage-dependent. Such a site may undergo a conformational change associated with inactiva-

tion. Pb^{2+} most likely binds to Ca^{2+} channels in the closed state and speeds the rate of inactivation.

Acknowledgments

The generous contribution of the Ca^{2+} channel cDNA clones by SIBIA Neurosciences, now Merck Research Laboratories, is gratefully acknowledged. Thanks are also due to Dr. Peter J. R. Cobbett (Department of Pharmacology and Toxicology, Michigan State University) for critical reading of the manuscript and valuable discussions.

References

Audesirk G (1993) Electrophysiology of lead intoxication: effects on voltage-sensitive ion channels. *Neurotoxicology* **14:**137–147.

Audesirk G and Audesirk T (1989) Effects of *in vitro* lead exposure on voltage-sensitive calcium channels differ among cell types in central neurons of *Lymnaea stagnalis Neurotoxicology* **10:**659–669.

Audesirk G and Audesirk T (1991) Effects of inorganic lead on voltage-sensitive calcium channels in N1E- 115 neuroblastoma cells. *Neurotoxicology* **12:**519–528.

Audesirk G and Audesirk T (1993) The effects of inorganic lead on voltage-sensitive calcium channels differ among cell types and among channel subtypes. *Neurotoxicology* **14:**259–265.

Axon Instruments (1994) *pClamp Users Guide*. p. 128, Foster City, CA.

Baukrowitz T and Yellen G (1995) Modulation of K^+ current by frequency and external $[K^+]$: a tale of two inactivation mechanisms. *Neuron* **15:**951–960.

Bernal J, Lee JH, Cribbs LL, and Perez-Reyes E (1997) Full reversal of Pb^{2+} block of L-type Ca^{2+} channels requires treatment with heavy metal antidotes. *J Pharmacol Exp Ther* **282:**172–180.

Bourinet E, Zamponi GW, Stea A, Soong TW, Lewis BA, Jones LP, Yue DT, and Snutch TP (1996) The α_{1E} calcium channel exhibits permeation properties similar to low-voltage-activated calcium channels. *J Neurosci* **16:**4983–4993.

Bourinet E, Stotz SC, Spaetgens RL, Dayanithi G, Lemos J, Nargeot J, and Zamponi GW (2001) Interaction of SNX482 with domains III and IV inhibits activation gating of α_{1E} (Ca(V)2.3)calcium channels. *Biophys J* **81:**79–88.

Brust PF, Simerson S, McCue AF, Deal CR, Schoonmaker S, Williams ME, Velicelebi G, Johnson EC, Harpold MM, and Ellis SB (1993) Human neuronal voltage-dependent calcium channels: studies on subunit structure and role in channel assembly. *Neuropharmacology* **32:**1089–1102.

Büsselberg D, Evans ML, Rahmann H, and Carpenter DO (1991) Lead and zinc block a voltage-activated calcium channel of *Aplysia* neurons. *J Neurophysiol* **65:**786–795.

Büsselberg D, Platt B, Michael D, Carpenter DO, and Haas HL (1994) Mammalian voltage-activated calcium channel currents are blocked by Pb^{2+}, Zn^{2+} and Al^{3+}. *J Neurophysiol* **71:**1491–1497.

Byerly L, Chase PB, and Stimers JR (1985) Permeation and interaction of divalent cations in calcium channels of snail neurons. *J Gen Physiol* **85:**491–518.

Cahill AL, Hurley JH, and Fox AP (2000) Coexpression of cloned α_{1B}, β_{2a} and $\alpha_2\delta$ subunits produces non-inactivating calcium currents similar to those found in bovine chromaffin cells. *J Neurosci* **20:**1685–1693.

Catterall WA (2000) Structure and regulation of voltage-gated Ca^{2+} channels. *Annu Rev Cell Dev Biol* **16:**521–555.

Choi KL, Aldrich RW, and Yellen G (1991) Tetraethylammonium blockade distinguishes two inactivation mechanisms in voltage-activated K^+ channels. *Proc Natl Acad Sci USA* **88:**5092–5095.

De Waard M and Campbell KP (1995) Subunit regulation of the neuronal α_{1A} Ca^{2+} channel expressed in *Xenopus* oocytes. *J Physiol* (*Lond*) **485:**619–634.

Evans ML, Büsselberg D, and Carpenter DO (1991) Pb^{2+} blocks calcium currents of cultured dorsal root ganglion cells. *Neurosci Lett* **129:**103–106.

Hamill OP, Marty A, Neher E, Sakmann B, and Sigworth FJ (1981) Improved patch-clamp techniques for high-resolution current recording from cells and cell-free membrane patches. *Pflueg Arch Eur J Physiol* **391:**85–100.

Hegg CC and Miletic V (1996) Acute exposure to inorganic lead modifies high-threshold voltage-gated calcium currents in rat PC12 cells. *Brain Res* **738:**333–336.

Hegg CC and Miletic V (1998) Diminished blocking effect of acute lead exposure on high-threshold voltage-gated calcium currents in PC12 cells chronically exposed to the heavy metal. *Neurotoxicology* **19:**413–420.

Hering S, Berjukow S, Sokolov S, Marksteiner R, Weiss RG, Kraus R, and Timin EN (2000) Molecular determinants of inactivation in voltage-gated Ca^{2+} channels. *J Physiol* **528:**237–249.

Hofmann F, Lacinova L, and Klugbauer N (1999) Voltage-dependent calcium channels: from structure to function. *Rev Physiol Biochem Pharmacol* **139:**33–87.

Hoshi T, Zagotta WN, and Aldrich RW (1990) Biophysical and molecular mechanisms of *Shaker* potassium channel inactivation. *Science (Wash DC)* **250:**533–538.

Kiss T and Osipenko ON (1994) Toxic effects of heavy metals on ionic channels. *Pharmacol Rev* **46:**245–267.

Liu Y, Jurman ME, and Yellen G (1996) Dynamic rearrangement of the outer mouth of a K^+ channel during gating. *Neuron* **16:**859–867.

Lopez-Barneo J, Hoshi T, Heinemann SH, and Aldrich RW (1993) Effects of external cations and mutations in the pore region on C-type inactivation of *Shaker* potassium channels. *Recept Channels* **1:**61–71.

Markovac J and Goldstein GW (1988) Picomolar concentrations of lead stimulate brain protein kinase C. *Nature (Lond)* **334:**71–73.

McEnery MW, Vance CL, Begg CM, Lee WL, Choi Y, and Dubel SJ (1998) Differential expression and association of calcium channel subunits in development and disease. *J Bioenerg Biomembr* **30:**409–418.

Mori Y, Friedrich T, Kim M, Mikami A, Nakai J, Ruth P, Bosse E, Hofmann F, Flockerzi V, Furuichi T, et al. (1991) Primary structure and functional expression from complementary DNA of a brain calcium channel. *Nature (Lond)* **350:**398–402.

Oortgiesen M, Leinders T, van Kleef RG, and Vijverberg HP (1993) Differential neurotoxicological effects of lead on voltage-dependent and receptor-operated ion channels. *Neurotoxicology* **14:**87–96.

Pan JQ and Lipscombe D (2000) Alternative splicing in the cytoplasmic II-III loop of the N-type Ca^{2+} channel α_{1B} subunit: functional differences are beta subunit-specific. *J Neurosci* **20:**4769–4775.

Parent L and Gopalakrishnan M (1995) Glutamate substitution in repeat IV alters divalent and monovalent cation permeation in the heart Ca^{2+} channel. *Biophys J* **69:**1801–1813.

Peng S-Q, Hajela RK, and Atchison WD (2001) Comparative effects of methylmercury, Hg^{2+} and Pb^{2+}on human neuronal α_{1B} and α_{1E} Ca^{2+} channels transiently expressed in human embryonic kidney cells in culture. *The Toxicologist* **60:**185.

Peng S-Q, Hajela RK, and Atchison WD (2002) Effects of methylmercury on human neuronal L-type calcium channels transiently expressed in human embryonic kidney cells. *J Pharmacol Expt Ther* **302:**424–432.

Reuveny E and Narahashi T (1991) Potent blocking action of lead on voltage-activated calcium channels in human neuroblastoma cells SH-SY5Y. *Brain Res* **545:**312–314.

Shafer TJ (1998) Effects of Cd^{2+}, Pb^{2+} and CH_3Hg^+ on high voltage-activated calcium currents in pheochromocytoma (PC12) cells: potency, reversibility, interactions with extracellular Ca^{2+} and mechanisms of block. *Toxicol Lett* **99:**207–221.

Simons TJ and Pocock G (1987) Lead enters bovine adrenal medullary cells through calcium channels. *J Neurochem* **48**:383–389.

Stea A, Tomlinson WJ, Soong TW, Bourinet E, Dubel SJ, Vincent SR, and Snutch TP (1994) Localization and functional properties of a rat brain α_{1A} calcium channel reflects similarities to neuronal Q- and P-type channels. *Proc Natl Acad Sci USA* **91:**10576–10580.

Sun LR and Suszkiw JB (1995) Extracellular inhibition and intracellular enhancement of Ca^{2+} currents by Pb^{2+} in bovine adrenal chromaffin cells. *J Neurophysiol* **74:**574–581.

Tomlinson WJ, Stea A, Bourinet E, Charnet P, Nargeot J, and Snutch TP (1993) Functional properties of a neuronal class C I-type calcium channel. *Neuropharmacology* **32:**1117–1126.

Tomsig JL and Suszkiw JB (1991) Permeation of Pb^{2+} through calcium channels: fura-2 measurements of voltage- and dihydropyridine-sensitive Pb^{2+} entry in isolated bovine chromaffin cells. *Biochim Biophys Acta* **1069:**197–200.

Tsien RW, Lipscombe D, Madison D, Bley K, and Fox A (1995) Reflections on Ca^{2+}-channel diversity, 1988–1994. *Trends Neurosci* **18:**52–54.

Williams ME, Feldman DH, McCue AF, Brenner R, Velicelebi G, Ellis SB, and Harpold MM (1992a) Structure and functional expression of α_1, α_2 and β subunits of a novel human neuronal calcium channel subtype. *Neuron* **8:**71–84.

Williams ME, Brust PE, Feldman DH, Patthi S, Simerson S, Maroufi A, McCue AF, Velicelebi G, Ellis SB, and Harpold MM (1992b) Structure and functional expression of an omega-conotoxin sensitive human N -type calcium channel. *Science (Wash DC)* **257:**389-#395.

Williams ME, Marubio LM, Deal CR, Hans M, Brust PF, Philipson LH, Miller RJ, Johnson EC, Harpold MM, and Ellis SB (1994) Structural and functional characterization of neuronal α_{1E} calcium channel subtypes. *J Biol Chem* **269:**22347–22357.

Woodhull AM (1973) Ionic blockage of sodium channels in nerve. *J Gen Physiol* **61:**687–708.

Yellen G, Sodickson D, Chen TY, and Jurman ME (1994) An engineered cysteine in the external mouth of a K^+ channel allows inactivation to be modulated by metal binding. *Biophys J* **66:**1068–1075.

Address correspondence to: Dr. Bill Atchison, Department of Pharmacology and Toxicology, Michigan State University, B-331 Life Sciences Bldg, East Lansing, MI 48824-1317. E-mail: atchiso1@msu.edu